Effect of the Chain Length on the Inter- and Intramolecular Dynamics of Liquid Oligo(ethylene glycol)s

Simon Schrödle, Richard Buchner,* and Werner Kunz

Institut für Physikalische und Theoretische Chemie, Universität Regensburg, D-93040 Regensburg, Germany

Received: December 19, 2003; In Final Form: March 17, 2004

Precise complex permittivity spectra over the frequency range 0.15 GHz $\leq \nu \leq$ 89 GHz are reported for monodisperse (EG_n, $1 \leq n \leq 6$) and polydisperse (PEG174, PEG300, PEG400) oligo(ethylene glycol)s at 25 °C. Up to about 20 GHz, the relaxation behavior of all samples can be reasonably described with empirical functions that reflect a broad and asymmetric relaxation time distribution, like the Havriliak−Negami function. However, these functions deviate systematically at higher frequencies and do not allow one to rationalize the concentration dependence of the spectra on dilution in dichloromethane or when going from the diol to the corresponding dimethyl ether. It is shown that a coherent description can be achieved by using a superposition of Debye-type relaxation processes. This approach allows the separation of end-group effects connected with the relaxation of the hydrogen bond network from intramolecular dipole relaxation processes caused by the reorientation of chain segments.

1. Introduction

Polymerization products of ethylene oxide, including poly(ethylene glycol)s (PEGs) and their alkyl ethers, are important bulk chemicals with a wide range of applications in the pharmaceutical, petroleum, cosmetic, textile, and other industries because of their good solubility in both water and organic solvents.[1,2] Additionally, oligo(ethylene glycol) chains are common hydrophilic moieties in nonionic surfactants and PEGs can, therefore, serve as model systems to investigate the properties of the hydrophilic parts of nonionic micelles and microemulsions[3,4] with implications for biological self-assembly processes.[2,5]

PEGs and their aqueous mixtures have been extensively studied with various techniques, such as IR,[6] NMR,[7−9] electron spin resonance,[9] or Raman spectroscopy,[10,11] by probing the Kerr effect,[12,13] and by different scattering techniques.[14,15] A common drawback of most investigations into the dynamic properties in the pure liquid state is the use of commercially available PEGs. Because of the methods used in their synthesis, those products are inherently polydisperse and represent mixtures of different homologues. This complicates the interpretation of the data because even the characterization of the material is difficult and physical parameters, like viscosity, can vary considerably with the supplier and the investigated batch.

There are some dielectric relaxation studies on pure PEGs[10,16−18] and their solutions,[16,19−24] but except for the atypical first member of the series, ethylene glycol,[25,26] data for the monodisperse oligo(ethylene glycol)s (EG_n, $H-(OC_2H_4)_n-OH$), are restricted to complex permittivity values, $\hat{\epsilon}(\nu) = \epsilon'(\nu) - i\epsilon''(\nu)$, at up to three different frequencies (ν) in the microwave region for tetra-, penta- and hexaethylene glycol.[27] These investigations revealed broad and unstructured complex permittivity spectra which could either be described as continuous relaxation time distributions or by sums of discrete Debye (D) type spectral components. $\hat{\epsilon}(\nu)$ is dominated by the cooperative dynamics of the intermolecular hydrogen bonds, but segmental motions involving the ether oxygens appear to become more important with increasing chain length. However, because of the largely differing frequency ranges covered by previous investigations and the general use of polydisperse samples, the appropriate description of the spectra and their interpretation in terms of inter- and intramolecular modes is still a matter of discussion.

This investigation aims at the separation of inter- and intramolecular effects on the dielectric relaxation behavior of EG_n and PEG compounds at 25 °C. On this behalf, $\hat{\epsilon}(\nu)$ was determined in the frequency range 0.15 GHz $\leq \nu \leq$ 89 GHz for monodisperse liquid oligo(ethylene glycol)s with polymerization degrees of $1 \leq n \leq 6$, for solutions of tri(ethylene glycol) in dichloromethane and for tri(ethylene glycol) dimethyl ether (EG_3Me_2). To study the effect of polydispersity and for comparison with literature data, PEGs with the average molecular weights of 174, 300, and 400 g mol^{-1} were investigated under the same conditions.

2. Experimental Section

Ethylene glycol (Aldrich, anhydrous, purity ≥99%, ≲50 ppm H_2O), tri(ethylene glycol) (Fluka, anhydrous, ≥99%, ≲265 ppm H_2O), penta(ethylene glycol) (Fluka, ≥97%, ≲1100 ppm H_2O), hexa(ethylene glycol) (Fluka, ≥97%, ≲880 ppm H_2O), tri(ethylene glycol) dimethyl ether (Merck, ≥98%, ≲500 ppm H_2O), and dichloromethane (Merck, ≥99%, ≲60 ppm H_2O) were used as delivered by the manufacturer. Di(ethylene glycol) (Aldrich, ≥99%, ≲150 ppm H_2O) and tetra(ethylene glycol) (Wako Pure Chemicals, ≥95%, ∼300 ppm H_2O) were purified and dried by fractional distillation at a reduced pressure (∼0.5 mbar) using a 40-cm vacuum-jacket Vigreux column.

PEGs with an average molar mass of $\bar{M} = 174$ (Wako PEG 200), 300 (Fluka), and 400 g mol^{-1} (Merck) were heated to about 100 °C until the vapor pressure dropped below ≈0.5 mbar. This treatment reduced the high water content in these materials to 890, 1400, and 400 ppm, respectively, without affecting the

* To whom correspondence should be addressed. E-mail: richard.buchner@chemie.uni-regensburg.de.

10.1021/jp037937h CCC: $27.50
Published on Web 04/23/2004

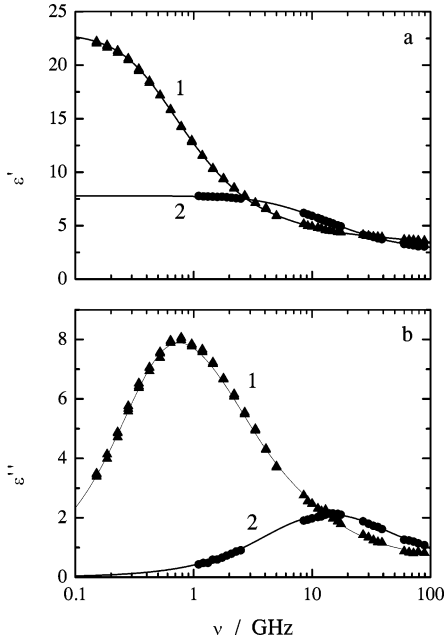

Figure 1. Dielelectric permittivity, $\epsilon'(\nu)$ (a), and loss, $\epsilon''(\nu)$ (b), of tri(ethylene glycol) (1) and tri(ethylene glycol) dimethyl ether (2) at 298.15 K.

molecular mass distribution. The unusal $\bar{M}$ of the first PEG (the sample of ref 10, donated by T. Matsouka and H. Nomura) results from the vacuum distillation of PEG 200 leading to an accumulation of components with low molecular mass compared with the mass distribution of the original material. $\bar{M} = 174$ g mol^{-1}, that is, an average polymerization degree of $\bar{n} = 3.54$, was determined from the refractive index (Zeiss, $\Delta n/n = 0.000\,05$, Na-D line, 25 ± 0.1 °C) using the data of Mori.[28] Evaluation of the static permittivity, ϵ, yielded $\bar{n} = 3.55$; see the following.

Samples were stored and handled in a dry nitrogen atmosphere to avoid water absorption from the environment. Water contents were determined by Karl Fischer titration. The densities of dichloromethane−tri(ethylene glycol) mixtures (Table 2) were obtained with a Paar DMA 60/601HT density meter at 25 ± 0.02 °C with an accuracy of ±0.1 kg m^{-3}.

Complex dielectric spectra were measured over the frequency range of 150 MHz to 89 GHz at 298.15 ± 0.05 K. At $\nu \lesssim 5$ GHz, data were recorded with a time-domain reflectometer using at least two cells of different cell constants to achieve an optimum signal-to-noise ratio.[29] Between 8.5 and 89 GHz, four waveguide interferometers based on the method of travelling waves were used.[30,31] Typical spectra obtained with this apparatus are shown in Figures 1 and 2.

3. Data Analysis and Results

For the interpretation of complex permittivity data, a mathematical model for the observed susceptibilities is needed. Usually, this is obtained by fitting sums

$$\hat{\epsilon}(\nu) = \sum_{j=1}^{l} S_j \tilde{F}_j(\nu) + \epsilon_\infty \qquad (1)$$

of l semiempirical band-shape functions $1 \le j \le l$, like the Havriliak−Negami (HN) equation[32,33]

$$\tilde{F}_j(\nu) = [1 + (\mathrm{i}2\pi\nu\tau_j)^{1-\alpha_j}]^{-\beta_j} \qquad (2)$$

or its variants (D, $\alpha_j = 0$, $\beta_j = 1$; Cole−Cole (CC), $0 < \alpha_j < 1$, $\beta_j = 1$; Cole−Davidson (CD), $\alpha_j = 0$, $0 < \beta_j < 1$) simultaneously to the real and imaginary part of the experimental complex permittivity data.[31,34] In eqs 1 and 2, τ_j is the relaxation time and $S_j = \epsilon_j - \epsilon_{j+1}$ is the amplitude (relaxation strength) of dispersion step j. The parameters α_j and β_j describe respectively a symmetrical and asymmetrical broadening of the corresponding band shape. ϵ_1 can be identified with the static permittivity, ϵ, of the sample. $\epsilon_\infty = \epsilon_{l+1}$ is the so-called infinite-frequency permittivity, here an adjustable parameter because the maximum frequency of these investigations, 89 GHz, does not cover the librational motions of the molecules.[34]

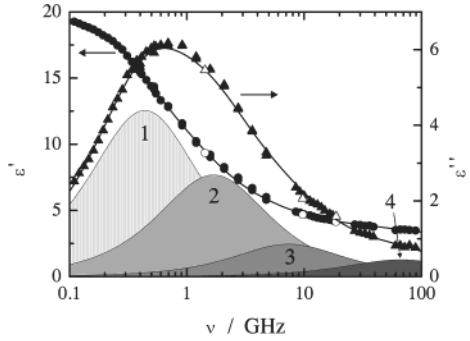

Figure 2. Spectrum of the dielectric permittivity, $\epsilon'(\nu)$ (●), and loss, $\epsilon''(\nu)$ (▲), of tetra(ethylene glycol) at 298.15 K. The solid lines are the sum of four D processes shown as individual contributions to ϵ'' by the shaded areas. Also included (open symbols) are the data of Koizumi[27] interpolated to 298.15 K.

For this investigation, all reasonable combinations of HN, D, CC, and CD equations for $1 \le l \le 5$ were simultaneously fitted to $\epsilon'(\nu)$ and $\epsilon''(\nu)$ using a computer program based on the Levenberg−Marquardt algorithm[37] and the obtained fits classified according to their reduced error function, χ_r^2,

$$\chi_r^2 = \frac{1}{2m-k} \sum_{i=1}^{m} [(\epsilon_i' - \epsilon_{i,\mathrm{ber}}')^2 + (\epsilon_i'' - \epsilon_{i,\mathrm{ber}}'')^2] \qquad (3)$$

where m is the number of measured frequencies and k is the number of adjustable parameters. In addition to the criterion of minimum variance, the selection of the most appropriate relaxation model was guided by the following criteria: (i) fit parameters must be physically meaningful, that is, fits with negative relaxation parameters or ϵ_∞ dropping below the square of the refractive index $(n_D^{25})^2$ were rejected; (ii) the number of adjusted parameters should be as small as possible; (iii) the relaxation model should not change within a series of measurements of homologous compounds or of the concentration dependence of mixtures except where physically reasonable; and (iv) within the series, parameters should vary smoothly (as defined by their error).

The data evaluation showed that for the pure oligo(ethylene glycol)s of polymerization degree $2 \le n \le 6$ as well as for the investigated commercial mixtures a sum of four D equations ($l = 4$, the 4D model) is most appropriate to describe $\hat{\epsilon}(\nu)$ in the measured frequency range. This is exemplified in Figure 2 for tetraethylene glycol, which also shows the contributions of the individual D processes to $\epsilon''(\nu)$. For some of the EG_n spectra, the relaxation behavior can also be described with similar χ_r^2 by using a single HN function or sums of CD and D functions. However, this partly leads to unphysical shape parameters (i.e., $\alpha < 0$) or to systematic deviations at high frequencies and, thus, such models do not allow a self-consistent interpretation of the EG_n series. For ethylene glycol ($n = 1$), a sum of three D equations (3D, $l = 3$) was sufficient. Because ethylene glycol

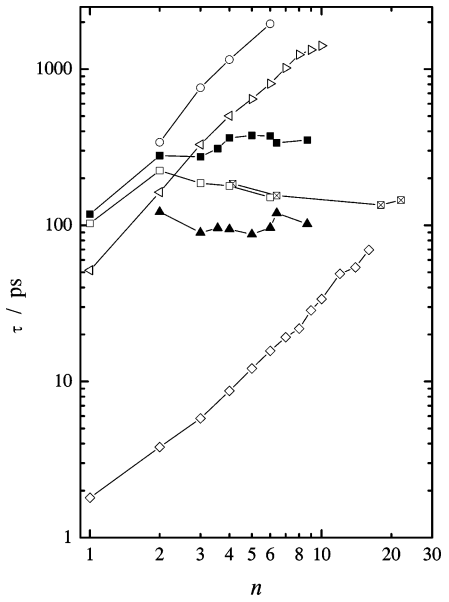

Figure 3. Relaxation times τ_1 (closed squares) and τ_2 (closed triangles) of this work and average relaxation times from the literature (open squares, ref 27; box with crosses, ref 16) of oligo(ethylene glycol)s, $H-(OC_2H_4)_n-OH$, as a function of the degree of oligomerization, n, at 298.15 K. For comparison, the τ_1 data of terminal n-diols $HO-(CH_2)_{n-1}-OH$ (open circles, ref 40), n-alcohols $CH_3(CH_2)_{n-1}-OH$ (left-pointing triangles, refs 25 and 41; right-pointing triangles, ref 42, 300 K), and n-alkyl bromides $CH_3(CH_2)_{n-1}-Br$ (diamonds, ref 43) with $n - 1$ methylene groups are shown at given n.

does not have C−O−C group-dipole moments like its higher homologues, the change of the relaxation model from 4D to 3D is reasonable and consistent with previous findings.[17] The parameters of the best fits are summarized in Table 1. The static permittivities thus obtained (column 2) for the pure EG_n compare well with capacitance-bridge data (column 12) from the literature.[35,36] Previous studies with more limited frequency coverage fitted a single CC equation to their data.[16,27] As can be seen from Figure 3, the relaxation times of these references are intermediate to the τ_1 and τ_2 values of this study and can be interpreted as weighted averages. The slight decrease of τ with increasing degree of oligomerization, n, suggested by the literature data is easily explained by the corresponding increase of amplitude S_2 relative to S_1; see Table 1. The results of Sengwa et al.[18] do not fit into the existing body of data. At 25 °C, all their static permittivities as well as the frequencies of maximum loss are significantly higher. A possible reason for this discrepancy might be contamination with water, which was not checked in ref 18.

The 4D model is also the most appropriate description for the spectra of EG_3/dichloromethane mixtures; see Table 2. Obviously, the dispersion step of CH_2Cl_2 centered around 65 GHz cannot be distinguished from the τ_4 mode of tri(ethylene glycol), and, thus, the amplitude $S_4 = \epsilon_4 - \epsilon_\infty$ is the sum of the solute and solvent contributions. On the other hand, the relaxation of tri(ethylene glycol) dimethyl ether differs markedly from the behavior of EG_3; see Figure 1. Firman et al. modeled their spectrum of EG_3Me_2 with a single CC equation.[39] For the present data, the CC model yielded similar parameters; see Table 3. However, the calculated $\epsilon''(\nu)$ depart significantly from the experimental data at low and high frequencies resulting in a large variance. The 2D model gives a considerable improvement but still shows systematic deviations. The best fit is obtained with the sum of a low-frequency CD and a high-frequency D equation (CD+D) or with a 3D model, which give equal χ_r^2. Interestingly, the relaxation times τ_1 and τ_2 of the CD+D and the 3D models are pretty similar, suggesting the physical relevance of these two modes. As discussed in the following, this is not so obvious for the process with $\tau_3 = 1.83$ ps suggested by the 3D fit.

TABLE 1: Relaxation Parameters ϵ_j and τ_j (in 10^{-12} s) and Reduced Error Functions, χ_r^2, of Pure Liquid Oligo(ethylene glycol)s with a Degree of Oligomerization $1 \le n \le 6$ for Fits with the 3D ($n = 1$) and 4D ($n > 1$, Mixtures), Respectively, Model at 298.15 K[a]

					EG_n						
n	ϵ_1	τ_1	ϵ_2	τ_2	ϵ_3	τ_3	ϵ_4	τ_4	ϵ_∞	χ_r^2	ϵ
1	40.23	118			6.94	14.3	4.74	1.82	3.54	0.0102	40.58
2	30.60	280	11.6	122	7.00	32.7	4.43	2.94	3.36	0.0167	30.75
3	23.00	274	11.0	89.7	5.62	18.2	4.00	2.08	3.12	0.0097	23.04
4	19.85	363	11.1	94.4	5.68	21.5	3.96	2.40	3.07	0.0100	19.90
5	17.21	376	10.8	87.5	4.80	11.1	3.53	1.04	2.78	0.0064	17.71
6	15.40	373	10.5	96.5	5.01	13.5	3.54	1.33	2.88	0.0087	15.59

					Mixtures						
$\bar{n}$	ϵ_1	τ_1	ϵ_2	τ_2	ϵ_3	τ_3	ϵ_4	τ_4	ϵ_∞	χ_r^2	$\bar{M}$
3.54	21.03	315	11.6	114	6.64	34.6	4.19	3.41	3.24	0.0057	174
6.40	14.77	337	10.9	120	5.81	23.3	3.80	2.58	3.03	0.0041	300
8.67	12.96	352	10.1	102	5.01	16.2	3.50	1.50	2.73	0.0026	400

[a] The same is presented for commercial mixtures of the average degree of oligomerization $\bar{n}$ and average molecular mass $\bar{M}$ (in g mol^{-1}).[35,36] For comparison, static permittivity data, ϵ, from the literature are included.

TABLE 2: Densities, ρ (in kg m^{-3}), and Relaxation Parameters ϵ_i and τ_i (in 10^{-12} s) of Solutions of Tri(ethylene glycol) of Mass Fraction w in Dichloromethane at 298.15 K Obtained with a 4D Model[a]

w	ρ	ϵ_1	τ_1	ϵ_2	τ_2	ϵ_3	τ_3	ϵ_4	τ_4	ϵ_∞	χ_r^2
0[b]	1316.3							9.20	2.07	2.45	
0.30	1254.5	13.44	112	12.5	39.7	7.83	7.63	5.72	2F	2.88	0.0036
0.45	1225.1	16.03	128	13.2	47.9	7.20	9.77	5.11	2F	2.89	0.0056
0.60	1196.3	18.24	138	11.9	50.2	6.30	9.95	4.50	2F	3.02	0.0078

[a] χ_r^2 is the reduced error function of the fit; parameters marked with "F" not adjusted. [b] Reference 38.

TABLE 3: Relaxation Parameters ϵ_j, τ_j (in 10^{-12} s), α_1, and β_1 and Reduced Error Function, χ_r^2, Obtained for Tri(ethylene glycol) Dimethyl Ether at 298.15 K with Different Relaxation Models[a]

model	ϵ_1	τ_1	α_1	β_1	ϵ_2	τ_2	ϵ_3	τ_3	ϵ_∞	χ_r^2
CC[b]	7.75	9.9	0.12	0					2.70	
CC	7.90	10.7	0.14	0					2.62	0.003 00
2D	7.77	17.59	0	0	4.68	4.56			2.71	0.001 73
CD+D	7.78	25.5	0	0.52	3.55	7.55			2.23	0.001 11
3D	7.78	22.2	0	0	5.76	8.01	3.26	1.83	2.56	0.001 06

[a] CC equation, superposition of two (2D) or three D equations (3D), and CD equation with an additional D term (CD+D). [b] Ref 39.

4. Discussion

Before going into a detailed comparison of the relaxation parameters of Tables 1−3 and their interpretation, it is important to reiterate that in none of examined cases the experimental $\hat{\epsilon}(\nu)$ spectrum can be reasonably fitted with a *single* semi-empirical relaxation-time distribution (band-shape function). Generally, the fit curves for models with $l = 1$ in eq 1 exhibit marked systematical deviations from the experimental data, even when using the rather flexible HN equation (CC and CD are even worse). More important, the ϵ_j and τ_j obtained for $l = 1$ models are not self-consistent for the investigated set of samples. A coherent set of relaxation parameters for all spectra, (i) pure EG_n as a function of chain length, (ii) tri(ethylene glycol)

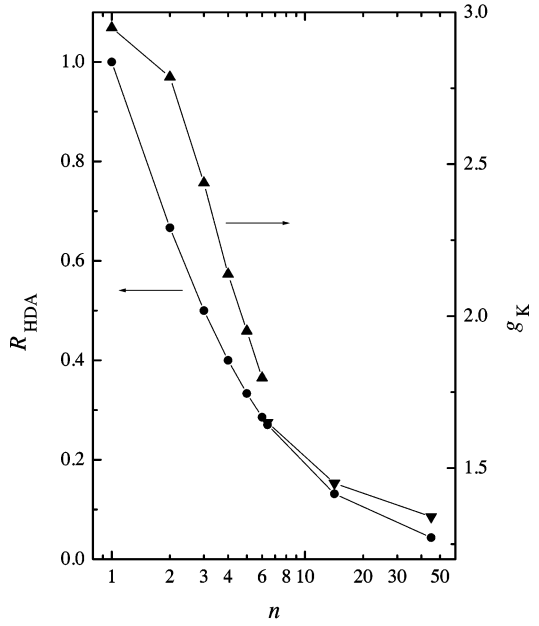

Figure 4. Kirkwood correlation factor, g_K, of oligo(ethylene glycol)s, EG_n, at 298.15 K as a function of the degree of oligomerization, n (▲, this work; ▼, ref 49). Also indicated is the ratio of H-bond donor to acceptor positions per molecule, R_{HDA} (●).

diluted in CH_2Cl_2, and (iii) pure tri(ethylene glycol) dimethyl ether, is only achieved for the multistep relaxation models worked out in the previous section (i, 4D; ii, 4D; iii, CD+D). As will be shown in the following, these multistep models can also be interpreted on a physically reasonable basis and conclusions can be linked to inference from other techniques.

The dielectric relaxation of tri(ethylene glycol) is strikingly different from the behavior of its dimethyl ether; see Figure 1. Compared with EG_3Me_2 (Table 3, column 2), the static permittivity of EG_3 is approximately tripled (Table 1) and the loss spectrum is dominated by a contribution at ~0.7 GHz. Similar differences are observed for the relaxation data of other oligo(ethylene glycol) dimethyl ethers and the corresponding diols of this investigation.

For the investigated EG_n, Loveluck[45] determined the dipole moment, μ_0, at infinite dilution in benzene. This allows the estimation of dipole−dipole correlations in the pure liquids with the help of the Kirkwood factor,

$$g_K = \mu_{eff}^2/\mu^2_0 \tag{4}$$

where μ_{eff} is the effective dipole moment of the sample calculated from the static, ϵ, and the infinite-frequency permittivity, ϵ_∞, with the Kirkwood−Fröhlich equation[46,47]

$$\frac{(\epsilon - \epsilon_\infty)(2\epsilon + \epsilon_\infty)}{\epsilon(\epsilon_\infty + 2)^2} = \frac{\rho'}{9\epsilon_0 k_B T}\mu_{eff}^2 \tag{5}$$

ϵ_0 is the permittivity of a vacuum, k_B is the Boltzmann constant, and T is the Kelvin temperature. The required number densities, ρ', were calculated from the data of Tawfik and Teja.[48] Because the ϵ_∞ of Table 1 still contain a contribution from librational motions, the common practice of setting $\epsilon_\infty \approx 1.1(n_D^{25})^2$ was followed. The required refractive indices at the sodium−D line, n_D^{25}, were taken from Mori.[28] Note that the choice of ϵ_∞ only shifts the magnitude of g_K but does not change the shape of $g_K(n)$.

The results are shown in Figure 4 together with Kirkwood factors (extrapolated to 298 K) determined by Kazbekov for several PEGs at their melting point.[49] g_K decreases with increasing degree of oligomerization, n, in a sigmoidal curve from ~2.95 for ethylene glycol to ~1.35 for $\bar{n} = 45$ to $g_K \approx 1.3$ at $\bar{n} = 150$.[49] Similar results were obtained by Loveluck at 293 K.[45] The difference in the Kirkwood factors of EG_3, $g_K = 2.3$, and its dimethyl ether, $g_K = 1.27$ (calculated from $\epsilon = 7.78$ and the data of refs 12, 50, and 51) is also significant, as well as the fact that the latter is close to the value approached by the PEGs at large n. Figure 4 also shows that the behavior of $g_K(n)$ is correlated with the ratio R_{HDA} of the H-bond donor to acceptor sites on the molecules. These observations suggest that from the two different kinds of dipolar groups (C−O−C within the chains and terminal C−O−H) present in these highly flexible molecules the C−O−C moieties are only weakly correlated in their relative inter- and intramolecular orientation despite a rotational barrier of 17 kJ mol^{-1} for the gauche−gauche transition.[7] Infrared studies of Kuroda and Kubo corroborate this conclusion.[6] On the other hand, C−O−H groups markedly enhance dipole−dipole correlations in these liquids as a result of the formation of inter- and intramolecular hydrogen bonds.

Except for ethylene glycol, EG_1, the relaxation time of the low-frequency process, τ_1 (Figure 3), is almost independent of the degree of oligomerization for $n \geq 2$ and no significant distinction can be found in the relaxation behavior of the investigated pure EG_n and the polydisperse PEGs (this applies to all ϵ_i and τ_i of Table 1). This observation, as well as the significantly smaller τ_1 value of EG_3Me_2 compared with EG_3 rule out rotational diffusion of the entire molecule to be the origin of the low-frequency dispersion of EG_n and PEGs. Note that the known flexibility of these molecules[6,7,52,54,55] would make such a rigid-rotor mode very unlikely anyway. Large values of τ_1 are typical for intermolecular hydrogen bonding because n-alcohols and terminal n-diols also exhibit large relaxation times in contrast to n-alkyl bromides (Figure 3). Commonly, the dominating low-frequency dispersion step of H-bonding liquids is assigned to the cooperative relaxation of the hydrogen-bond system and assumed to involve a dwelling time for the bond-breaking step of a molecule and a subsequent waiting time for the reformation of a H bond by this molecule with a new partner.[40,42,56−60] In the case of water, hydrogen bond breaking appears to be rate-determining for τ_1.[61] But similar to n-alcohols[42,57] and terminal n-diols,[40] the availability of an appropriate neighbor should be more important for the investigated glycols as a result of the reduced donor-to-acceptor ratio. This is corroborated by the plot of τ_1 versus the concentration of oxygen atoms (H-bond acceptor sites), c_O, in Figure 5 which shows that τ_1 increases exponentially with decreasing c_O. Interestingly, the EG_n are in line with the structurally related terminal diols and H_2O, whereas the n-alcohols form a separate line of a different slope and relax by approximately 1 order of magnitude faster for a given c_O. Possibly, the two correlations reflect the different structures of these liquids, that is, winding chains in the case of the alkanols due to a single H-bond donor group per molecule and cross-linked networks for the diols and EG_n with two donor groups. Figure 5 also explains why for the EG_n and PEGs with ≥2 the cooperative relaxation time τ_1 remains almost unchanged: the number density of oxygen sites, c_O, rapidly approaches a saturation value of ~27.5 mol L^{-1}.

The relative amplitude (strength) of the low-frequency dispersion, $S_1^r = (\epsilon_1 - \epsilon_2)/(\epsilon_1 - \epsilon_\infty)$, decreases markedly with n, but this essentially reflects the decreasing dipole density. It is more instructive to scale S_1^r (and the other relative amplitudes) to the concentration of the glycol, c; see Figure 6. In this plot,

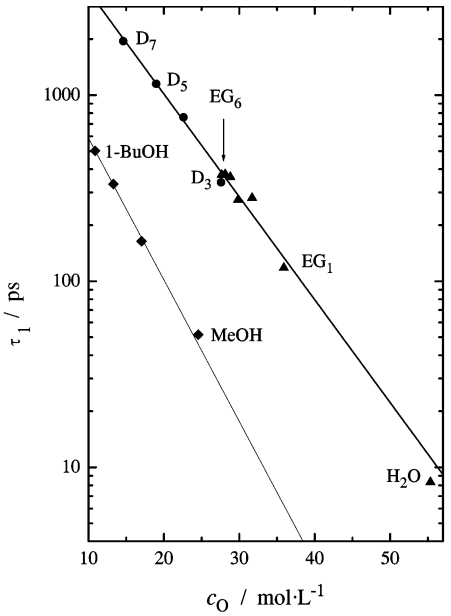

Figure 5. Relaxation time τ_1 as a function of the concentration of oxygen sites (H-bond acceptor sites), c_O, for water and the oligo(ethylene glycol)s EG_1-EG_6 (▲); for *n*-alkanols from methanol to 1-butanol (◆, data from refs 26 and 41); and for terminal *n*-diols,[40] D_i, with $i = 3-5$ and 7 methylene groups (●) at 298.15 K.

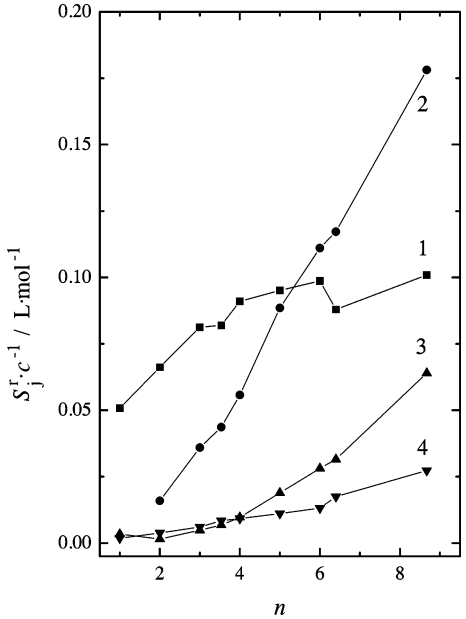

Figure 6. Relative disperson amplitudes, S_1^r (■), S_2^r (●), S_3^r (▲), and S_4^r (▼) of oligo(ethylene glycol)s, EG_n, of the degree of oligomerization, *n*, normalized to the EG_n concentration, *c*, at 298.15 K.

$S_1^r c^{-1}$ increases moderately at low *n* and then seems to level off. Because *c* is 1/2 the concentration of the OH groups, this means that in the pure oligo(ethylene glycol)s the fluctuation of the macroscopic dipole moment per H-bond donor unit that is associated with the cooperative relaxation reaches a saturation value. On the other hand, $S_1^r c^{-1}$ decreases markedly for EG_3 on dilution in dichloromethane for EG_3 mole fractions $x < 0.45$ ($w < 0.6$; Figure 7), and, simultaneously, the cooperative dynamics speeds up (column 2 of Table 2). It is well-known not only that with increasing chain length packing requirements enforce a more and more pronounced parallel alignment of the oligomer backbones[13,55] but also that PEGs self-associate in concentrated nonaqueous solutions.[7] Thus, curves 1 in Figures 6 and 7 suggest that for chain lengths of $n \gtrsim 4$ intermolecular

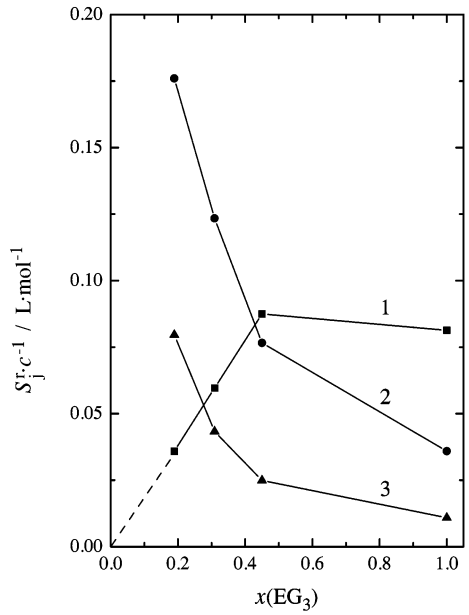

Figure 7. Relative dispersion amplitudes, S_1^r (■), S_2^r (●), and S_3^r (▲) of tri(ethylene glycol) in mixtures with dichloromethane, normalized to the concentration of EG_3, *c*, as a function of the mole fraction $x(EG_3)$ at 298.15 K.

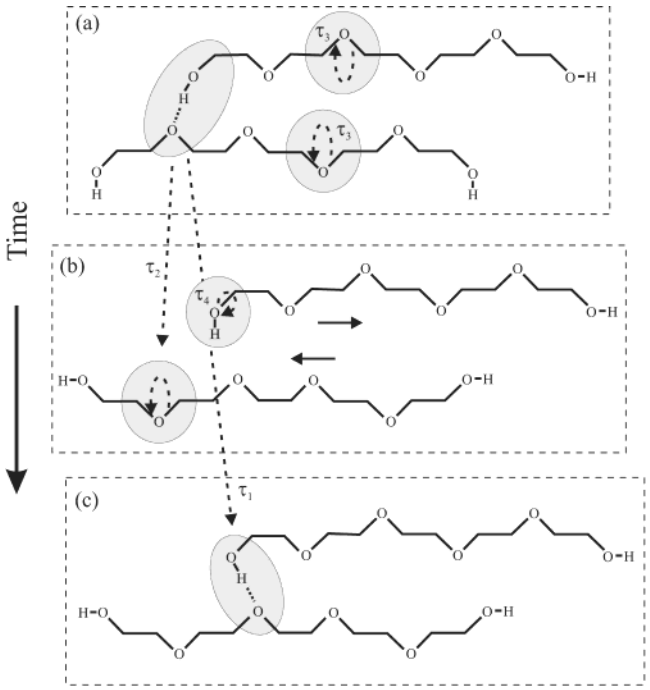

Figure 8. Possible molecular motions connected with the relaxation times $\tau_1-\tau_4$ of oligo(ethylene glycol)s. See text for explanation.

hydrogen bonds between the terminal donors and −C−O−C− acceptor sites predominate in pure PEGs and the low-frequency relaxation involves a kind of motion which is independent of *n*. It is tempting to assume for this mode a hopping of the hydrogen-bonding OH group of a donor molecule along the ether oxygens of the accepting neighbor, as sketched in Figure 8. On the other hand, at shorter chain lengths less extensive molecular motions may be required for the cooperative mode in the pure liquids because of the larger density of donor sites and a larger contribution of terminal −C−O−H groups simultaneously acting as acceptors. The marked decrease of $S_1^r c^{-1}$ on dilution below a certain threshold concentration of EG_3 in dichloromethane indicates the breakup of the H-bonded

aggregates at $x < 0.45$. Possibly, this is accompanied by the formation of intramolecular H bonds that leads to the observed decrease of τ_1, because from the decreasing concentration of oxygen sites an increase of τ_1 similar to methanol/tetrachloromethane mixtures[58] would be expected.

A fast mode of small amplitude, with a relaxation time on the order of 0.3−2 ps, is a common feature of the dielectric relaxation of water, alcohols, and their mixtures, see, for example, refs 41 and 60−62, and apparently associated with the fast rotation of non-hydrogen-bonded OH groups. For the investigated EG_n and PEGs, such a mode is possible, see Figure 8, and τ_4 (column 9 of Table 1) has the appropriate magnitude (for the EG_3/CH_2Cl_2 mixtures, Table 2, this mode is superimposed by the relaxation of dichloromethane and, thus, will not be discussed). However, this cannot be the only contribution to S_4 because curve 4 of Figure 6 shows an increase of $S_4^r c^{-1}$ with increasing chain length, n, although the OH concentration decreases. It could be argued that this reflects a decrease of the degree of hydrogen bonding, but because the ratio of H-bond acceptors to donors, c_O/c_{OH}, increases with n, this explanation seems very unlikely. A hint is given by the fit data for EG_3Me_2, Table 3. This compound does not have OH groups. Nevertheless, it is possible to fit a 3D model to $\hat{\epsilon}(\nu)$, yielding a fast dispersion step with $\tau_3 = 1.83$ ps (corresponding to a peak frequency of 87 GHz) and $S_3^r = 0.13$. This suggests that for the ether and consequently also for the glycols fast intramolecular segmental motions of the molecules contribute to $\hat{\epsilon}(\nu)$ up to at least 89 GHz (the maximum frequency of our experiments) and become more important with increasing chain length.

The relaxation time of the slowest process of EG_3Me_2, $\tau_1 \approx 24$ ps (Table 3, column 3) obtained with the CD+D and the 3D models, is similar to data of poly(oxyethylene) dimethyl ethers, like PEO-500 ($\tau \approx 40$ ps).[44,53] It is typical for the segmental motion of oxyethylene chains connected with the reorientation of the dipolar C−O−C units around the C−C bonds; see Figure 8.[54] For EG_3Me_2, an assignment of the (S_1, τ_1) dispersion to this "crankshaft motion" of the oligomer backbone appears, thus, reasonable. The relaxation time τ_3 of the EG_n and PEGs (Table 1, column 7), in the range of 10−35 ps, is similar to the time constant of the "crankshaft motion". The associated concentration-corrected relative amplitude, $S_3^r c^{-1}$, increases with chain length n (Figure 6) and for EG_3 on dilution in dichloromethane (Figure 7). Both observations are, therefore, in line with an assignment of the (S_3, τ_3) mode to the intramolecular motion of C−O−C units which are not involved in hydrogen bonds. In the first case, the ratio of H-bond donors to acceptors decreases and with increasing n more and more unoccupied C−O−C sites will be present, whereas upon sufficient dilution the intermolecular interaction of the EG_3 molecules will be suppressed. The EG_3Me_2 dispersion step with $\tau_2 \approx 7.7$ ps might be connected with the reorientation of the terminal methyl ether groups because dimethoxy ethane (where the "crankshaft motion" is not possible) has a comparable relaxation time of 4.5 ps.[63]

For the pure glycols, the relaxation time of the (S_2, $\tau_2 \approx 100$ ps) mode is essentially constant (Table 1 for $n \geq 2$, but its concentration-corrected relative amplitude, $S_2^r c^{-1}$, increases considerably and practically linearily (curve 2 of Figure 6). Most straightforward is the assignment of this mode to the intramolecular reorientation of C−O−C groups that are involved in hydrogen bonds; see Figure 8. The requirement of breaking the H bond before the C−O−C rotation can take place explains the fairly large τ_2. Such a mode is not possible for ethylene glycol (where no such process is detected). This process is also not very important at small n as a result of the comparable number of ether and alcohol oxygens, that is, of internal and terminal acceptor sites. But with increasing n the probability of a H-bond donor to bind to an ether oxygen increases considerably because this is enhanced by the observed backbone alignment.[13] Obviously, this explanation cannot hold for the increase of $S_2^r c^{-1}$ on dilution of EG_3 in dichloromethane (Figure 7). Maybe the dilution effect arises from increased intramolecular hydrogen bonding accompanied by more rapid intramolecular dynamics (suggested by the decreasing relaxation times τ_1, τ_2, and τ_3; Table 2).

5. Conclusions

The dielectric relaxation of oligo(ethylene glycol)s in the pure state and diluted in an "inert" solvent, as well as the complex permittivity spectra of the corresponding dimethyl ethers (with EG_3Me_2 as the example) are best fitted by sums of D equations. It is shown in this contribution that such a formal description allows a self-consistent assigment of the resolved dispersion steps to modes of inter- and intramolecular motions and interactions; see Figure 8. Namely, for the glycols the (S_1, $\tau_1 \approx 300$ ps) mode can be associated with the cooperative intermolecular dynamics of the terminal C−O−H groups acting as a H-bond donor or acceptor; (S_2, $\tau_2 \approx 100$ ps) reflects the dynamics of the ether oxygens involved as acceptors in hydrogen bonds; (S_3, $\tau_3 \approx 20$ ps) is connected with the "crankshaft motion" of free C−O−C groups; and (S_4, $\tau_4 \approx 2$ ps) is connected with the reorientation of non-hydrogen-bonded O−H groups. This interpretation not only fits into the picture emerging for the dielectric relaxation of hydrogen-bonding liquids over the last years[40,42,56−60] but also is consistent with results from other experimental techniques and computer simulations. Additionally, from the observed 4D relaxation model it can be understood why polydispersity is not significant for the dielectric relaxation behavior of PEGs. Fits with one of the commonly used continuous relaxation time distributions, like the HN or the Kohlrausch−Williams−Watts equation, generally do not give such good fits, nor are the results self-consistent for the investigated series of samples.

Nevertheless, the 4D scenario sketched in Figure 8, as appealing as it is, should be taken with a grain of salt. The model certainly grasps essential features of the complex cooperative and molecular dynamics of oligo(ethylene glycol)s which definitely cannot be approximated by a single HN equation or similar simple empirical approaches. However, the suggested inter- and intramolecular motions are not independent of each other and, thus, the 4D model is only approximation. Although the correlation length for the "unperturbed" crankshaft motion, (S_3, τ_3), appears to be short, the influence of H-bonded neighbors cannot be neglected because at least for short-chain EG_n the probability to have an H-bonded C−O−C or C−O−H group nearby is overwhelming. This applies also for the other modes; see especially the discussion of the (S_4, τ_4) relaxation. A continuous distribution of relaxation times, $G(\ln \tau)$, with maxima or at least shoulders at the τ_j of the 4D model, is certainly more appropriate for these liquids of highly flexible molecules. The systematic deviation of $\epsilon''(\nu)$ around 1.5 GHz for EG_4 (Figure 2) which, to a lesser extent, is also present in the spectra of the other oligo(ethylene glycol)s, may be a hint at such a distribution. However, more accurate measurements than currently feasible in the gigahertz range and probably assistance by molecular dynamics simulations are required to extract the "true" $G(\ln \tau)$.

References and Notes

(1) *Water Soluble Polymers, Synthetic Polymers: Properties and Uses*; Molyneux, P., Ed.; CRC Press: Boca Raton, FL, 1983.

(2) Harris, J. M. *Poly(Ethylene Glycol) Chemistry: Biotechnical and Biomedical Applications*; Plenum Press: New York, 1992.

(3) Sjöblom, J.; Stenius, P.; Danielsson, I. In *Nonionic Surfactants*; Schick, M. J., Ed.; Marcel Decker: New York, 1987.

(4) Laughlin, R. G. *The Aqueous Phase Behaviour of Surfactants*; Academic Press: London, 1994.

(5) Fleming, K. G. *Curr. Opin. Biotechnol.* **2000**, *11*, 67.

(6) Kuroda, Y.; Kubo, M. *J. Polym. Sci.* **1957**, *26*, 323.

(7) Liu, K.-J.; Ullman, R. *J. Chem. Phys.* **1968**, *48*, 1158.

(8) Matsuzaki, K.; Ito, H. *J. Polym. Sci.* **1974**, *12*, 2507.

(9) Lang, M.-C.; Laupretre, F.; Noel, C.; Monnerie, L. *J. Chem. Soc., Faraday Trans. 2* **1979**, *75*, 349.

(10) Nomura, H.; Koda, S.; Matsuoka, T.; Noudou, T.; Buchner, R.; Barthel, J. *J. Mol. Liq.* **1998**, *78*, 29.

(11) Tasaki, K. *Polym. Mater. Sci. Eng.* **1995**, *73*, 12.

(12) Khanarian, G.; Tonelli, A. E. *Macromoleules* **1982**, *15*, 145.

(13) Drozdowski, A.; Błkaszczak, Z.; Iwaszkiewicz-Kostka, I.; Ziobrowski, P.; Andrzejewska, E.; Andrzejewski, M. *J. Mol. Struct.* **2002**, *614*, 47.

(14) Branca, C.; Magazu, S.; Maisano, G.; Migliardo, F.; Migliardo, P.; Romeo, G. *J. Phys. Chem. B* **2002**, *106*, 10272.

(15) Dahlborg, U.; Dimic, V. *Phys. Scr.* **1988**, *37*, 93.

(16) Davies, M.; Williams, G.; Loveluck, G. D. *Z. Elektrochem.* **1960**, *64*, 575.

(17) Utzel, H.; Wessling, E.; Dachwitz, E.; Stockhausen, M. *Colloid Polym. Sci.* **1990**, *268*, 330.

(18) Sengwa, R. J.; Kaur, K.; Chaudhary, R. *Polym. Int.* **2000**, *49*, 599.

(19) Kaatze, U.; Göttmann, O.; Podbielski, R.; Pottel, R.; Terveer, U. *J. Phys. Chem.* **1978**, *82*, 112.

(20) Kaatze, U. *Ber. Bunsen-Ges. Phys. Chem.* **1978**, *82*, 690.

(21) Kaatze, U. *Colloid Polym. Sci.* **1978**, *65*, 214.

(22) Wessling, E.; Stockhausen, M.; Schütz, G. *J. Mol. Liq.* **1991**, *49*, 105.

(23) Kaatze, U.; Lönnecke-Gabel, V.; Pottel, R. *Z. Phys. Chem. NF* **1992**, *175*, 165.

(24) Salomon, M.; Xu, M.; Eyring, E. M.; Petrucci, S. *J. Phys. Chem.* **1994**, *98*, 8234.

(25) Angell, C. A.; Smith, D. L. *J. Phys. Chem.* **1982**, *86*, 3845.

(26) Pickl, H. Ph.D. Thesis, Universität Regensburg, Regensburg, Germany, 1998.

(27) Koizumi, N. *J. Chem. Phys.* **1957**, *27*, 625.

(28) Mori, S. *Anal. Chem.* **1978**, *50*, 1639.

(29) Buchner, R.; Barthel, J. *Ber. Bunsen-Ges. Phys. Chem.* **1997**, *101*, 1509.

(30) Barthel, J.; Bachhuber, K.; Buchner, R.; Hetzenauer, H.; Kleebauer, M. *Ber. Bunsen-Ges. Phys. Chem.* **1991**, *95*, 853.

(31) Barthel, J.; Buchner, R.; Eberspächer, P.-N.; Münsterer, M.; Stauber, J.; Wurm, B. *J. Mol. Liq.* **1998**, 78, 82.

(32) Havriliak, S.; Negami, S. *J. Polym. Sci., Part C* **1966**, *14*, 99.

(33) *Broadband Dielectric Spectroscopy*; Kremer, F., Schönhals, A., Eds.; Springer: Berlin, 2002.

(34) Barthel, J.; Buchner, R.; Münsterer, M. In *Electrolyte Data Collection, Part 2: Dielectric Properties of Water and Aqueous Electrolyte Solutions*; Kreysa, G., Ed.; Chemistry Data Series; DECHEMA: Frankfurt, 1995; Vol. XII.

(35) Koizumi, N.; Hanai, T. *J. Phys. Chem.* **1956**, *60*, 1496.

(36) Barthel, J.; Neueder, R.; Schröder, P. In *Electrolyte Data Collection, Part 1b: Conductivities, Transference Numbers, and Limiting Ionic Conductivities of Solutions of Propanol, Butanol, and Higher Alcohols*; Kreysa, G., Ed.; Chemistry Data Series; Dechema: Frankfurt, 1994; Vol. XII.

(37) Bevington, P. R. *Data Reduction and Error Analysis for the Physical Sciences*; McGraw-Hill: New York, 1969.

(38) Vij, J. K.; Hufnagel, F.; Grochulski, T. *J. Mol. Liq.* **1991**, *49*, 1.

(39) Firman, P.; Xu, M.; Eyring, E. M.; Petrucci, S. *J. Phys. Chem.* **1993**, *97*, 3606.

(40) Wang, F.; Pottel, R.; Kaatze, U. *J. Phys. Chem. B* **1997**, *101*, 922.

(41) Barthel, J.; Bachhuber, K.; Buchner, R.; Hetzenauer, H. *Chem. Phys. Lett.* **1990**, *165*, 369.

(42) Mandal, H.; Frood, D. G.; Saleh, M. A.; Morgan, B. K.; Walker, S. *Chem. Phys.* **1989**, *134*, 441.

(43) Hennelly, E. J.; Heston, W. H.; Smyth, C. P. *J. Am. Chem. Soc.* **1948**, *70*, 4102.

(44) Borodin, O.; Douglas, R.; Smith, G.; Eyring, E. M.; Petrucci, S. *J. Phys. Chem. B* **2002**, *106*, 2140.

(45) Loveluck, G. D. *J. Chem. Soc.* **1961**, 4729.

(46) Kirkwood, J. G. *J. Chem. Phys.* **1939**, *7*, 911.

(47) Fröhlich, H. *Theory of Dielectrics*, 2nd ed.; Oxford University Press: Oxford, 1958.

(48) Tawfik, W. Y.; Teja, A. S. *Chem. Eng. Sci.* **1989**, *44*, 921.

(49) Kazbekov, A. G. *Vliyanie Fiz. Protsessov na Kalii-argonov. Vozrast Mineralov* **1981**, 108.

(50) Pal, A.; Singh, Y. P. *J. Chem. Eng. Data* **1996**, *41*, 1008.

(51) Pal, A.; Dass, G.; Kumar, A. *J. Chem. Eng. Data* **1998**, *43*, 738.

(52) Smith, G. D.; Yoon, D. Y.; Jaffe, R. L.; Colby, R. H.; Krishnamoorti, R.; Fetters, L. J. *Macromolecules* **1996**, *29*, 3462.

(53) Borodin, O.; Douglas, R.; Smith, G. D.; Trow, F.; Petrucci, S. *J. Phys. Chem. B* **2003**, *107*, 6813.

(54) Smith, G. D.; Yoon, D. Y.; Wade, C. G.; O'Leary, D.; Chen, A.; Jaffe, R. L. *J. Chem. Phys.* **1997**, *106*, 3798.

(55) Livadaru, L.; Netz, R. R.; Kreuzer, H. J. *J. Chem. Phys.* **2003**, *118*, 1404.

(56) Kaatze, U.; Pottel, R. *J. Mol. Liq.* **1992**, *52*, 181.

(57) Kaatze, U.; Behrends, R.; Pottel, R. *J. Non-Cryst. Solids* **2002**, *305*, 19.

(58) Buchner, R.; Barthel, J. *J. Mol. Liq.* **1992**, *52*, 131.

(59) Buchner, R.; Hölzl, C.; Stauber, J.; Barthel, J. *Phys. Chem. Chem. Phys.* **2002**, *4*, 2169.

(60) Sato, T.; Buchner, R. *J. Chem. Phys.* **2003**, *119*, 10789.

(61) Buchner, R.; Barthel, J.; Stauber, J. *Chem. Phys. Lett.* **1999**, *306*, 57.

(62) Rønne, C.; Thrane, L.; Åstrand, P.-O.; Wallqvist, A.; Mikkelsen, K. V.; Keiding, S. R. *J. Chem. Phys.* **1997**, *107*, 5319.

(63) Farber, H.; Petrucci, S. *J. Phys. Chem.* **1981**, *85*, 2987.